A MICROMECHANICAL MODEL OF ASR ANISOTROPY. APPLICATION TO AFFECTED COLUMNS.

Laurent Charpin*

EDF R&D, Department of Mechanics and Materials of Components, Ecuelles, FRANCE

Abstract

Alkali Silica Reaction induces microscopic cracking which reduces the mechanical properties of affected concrete, and leads to macroscopic swelling. Under anisotropic loading, swelling and cracking are also anisotropic.

This paper presents a model that aims at simulating the development of cracking at the microscopic scale. A micromechanical description of the concrete and an energy fracture criterion are used in this purpose. The model parameters have been identified on laboratory experiments of ASR under loading. The results are considered satisfactory up to loadings of 10 MPa.

Finally, the model is used to assess the safety of 18 m high and 70 cm wide columns showing signs of chemical internal swelling, in a nuclear power plant operated by EDF in France. The model provides valuable information about the length change of the columns depending on the vertical load applied. The results helped taking important decisions about the rehabilitation procedures which are currently undertaken in EDF maintenance strategy.

Keywords: ASR, anisotropy, energy criterion, poromechanics, field application

1 INTRODUCTION

Alkali-silica reaction can affect concrete containing aggregates with reactive silica, with a high alkali content, and exposition to water. This chemical reaction dissolves amorphous parts of the aggregates, first inducing a reduction of their densities. Then, the dissolved silica combines with alkali, forming a hydrophilic gel which can swell due to water absorption. Calcium can also enter in the composition of this gel. Therefore, a very wide range of products can be formed depending on the relative amounts of silica, alkali and calcium available in the system. They can be formed in different locations depending on the aggregate type [1]. The link between the composition of the products and the swelling capacity is still not fully clear. Even though some models attempt to predict the amount of gel created (e.g. [2]), a model able to predict the location of the gel creation still does not exist.

The macroscopic consequences of ASR are swelling and cracking which need to be predicted for safety and operational reasons. When large structures such as bridges, dams, or nuclear power plants show signs of ASR, it is important to estimate the remaining time during which the structure can be used safely. The mechanical modelling of ASR has been the focus of many researchers in the past two decades. Some models based on FE codes are designed for the computation of large structures (e.g. [3], [4]). They simulate deformations due to ASR along with creep and damage. The difficulty is the large number of parameters of such models. These parameters require a large number of complex experiments to be identified for each case of study.

In this work, one attempts to improve the mechanical description of cracking during ASR, following the work of Bažant et al. [5]. This model was initially developed for waste glass, which is comparable to fast-reacting aggregates [1]. Hence, the damage mechanism modeled here is more appropriate to describe ASR in fast-reacting aggregates, and should be extended to include the case of slowly reactive aggregates, for which cracking is first observed inside the aggregate particles, where the gel is initially located, before it extends to cement paste [6] [7]. Despite this intrinsic limitation of the model, this assumption is found to be efficient in representing the anisotropic expansion of concrete under loading, in experiments performed by Multon [8]. In these experiments, the reactive aggregates used were limestone crushed aggregates with silica whitish veins. One thinks that due to the presence of such whitish veins, the gel the cracks filled with gel can reach either the cement paste or outline the aggregate particles and thus filling the ITZ.

Finally, one uses the model for a particular case at EDF. Reinforced concrete columns which are part of the cooling tower of a nuclear plant in France were thought to be affected by a swelling reaction due to observations of visible cracks. The potential failure of one of these columns could

* Correspondence to: laurent.charpin@edf.fr

make the cooling tower unavailable for a long period of time, which could be extremely costly to the company. Therefore, studies as well as rehabilitation procedures were undergone. The model presented is applied to the case of these columns despite the doubts existing about the fact that the chemical reaction might be partially delayed ettringite formation (DEF) instead of pure ASR. Even if the application of the model has likely defaults which are discussed in the following sections, it still yields valuable information about the difference of strains of columns submitted to different loading levels, and the possible decrease of the Young's moduli of the affected concrete. Finally, the mechanical effect of reinforcing the columns with fiber reinforced composites (FRC) is discussed.

2 MICROMECHANICAL MODEL FOR ASR ANISOTROPY

The anisotropy of ASR under loading, as explained by Hobbs [9], was first observed on loaded structures, through the preferential orientation of the macroscopic cracks. These cracks appear due to the fact that the surface of structures usually swells less than their core, because of the lack of water, and also because of alkalis leaching. The direction of these cracks reflects the swelling occurring in the core of the structure, and they tend to align with the main compression direction.

Although anisotropy also exists in unloaded specimens, due to preferential aggregate orientation for example, a large part of anisotropy is due to the orientated growth of microcracks under loading [9]. The idea behind the present model is that since cracks propagate under the combined action of gel pressure within concrete porosity and external loading, it is possible to predict the direction of appearance of the cracks using a very schematic description of the concrete microstructure and the crack propagation, through micromechanics, and an energy criterion for the propagation of cracks.

This model has been extensively described in the author's PhD thesis [10], in French, and in a journal article [11]. Therefore, only the main features of the model will be presented here.

2.1 Morphological description of the concrete under attack

We have chosen to represent concrete as a composite material made of aggregates surrounded by an ITZ and embedded in a cement paste matrix. The radii of aggregates can vary by many orders of magnitude, which makes the micromechanical description very useful. Indeed, the explicit definition, meshing and FE computations of a 3D representative volume element of such a material requires heavy computational tools. The aggregate inside is separated in two zones: a sound zone where alkali have not reached (and thus dissolution has not started), and an attacked zone, where the amorphous silica has been dissolved, as illustrated in Figure 1.

Each aggregate of size R^i is surrounded by an ITZ of thickness l_c. While the porosity of the cement paste matrix is not taken into account, the ITZ is considered porous, of porosity ρ_{itz}. Its mechanical behaviour is assumed to be poroelastic. The role of this porosity is to act as a reservoir for the gel, which is either expelled from the aggregate due to a lack of space, or formed directly in the ITZ. It also plays a mechanical role, reducing slightly the overall concrete stiffness due to its high porosity compared to the cement paste.

While the sound zone is linear elastic, the attacked zone is poroelastic with porosity ρ_i. The value of this porosity depends on the amount of reactive silica inside the aggregate particles under consideration, and can be different from one aggregate class to another.

The gel, which is formed in the new porosity of the attacked zone or in the ITZ, has a volume which is larger than the dissolved aggregate volume. This volume ratio is called $\delta > 1$. Hence, a pressure build-up occurs. One could imagine that it first leads to cracking of the aggregate which would be more appropriate for the description of slow reactive aggregates. At the moment, this mechanism is not implemented. Instead, the model assumed that the first crack occurs at the ITZ, causing a decohesion between the aggregate particle and the cement paste. Second, if the gel pressure still progresses, a second mechanism can start: cracking in the cement paste. We assume that three annular cracks can appear around the aggregate, as shown on Figure 2.

Hence, we see that we need a procedure to compute the propagation of the cracks: first decohesion and then increase of the crack sizes x_1^i, x_2^i, x_3^i for each aggregate class i, starting from the knowledge of the gel expansion ratio δ and the progress of the dissolution front $\alpha^i(t)$.

2.2 Poromechanical description

The attacked concrete is submitted to an external loading: imposed stress, imposed strain, or both depending on the direction considered. At the same time, the attack induces pressure p^i in the aggregate class i. A given aggregate class is considered as a whole, without explicit description of

particular aggregates. Therefore, aggregates which are gathered in a given family will undergo the same evolution of attack depth $\alpha^i(t)$, pressure, and cracking. Therefore, without loss of generality, the behaviour of the concrete at the macroscopic scale can be written:

$$(1)\quad \begin{cases} \underline{\underline{\Sigma}} = \mathbb{C}^{hom} : \underline{\underline{E}} - \sum_{i=1}^{N_f} p^i \underline{\underline{B}}^i \\ \varphi^i - f^i = \underline{\underline{B}}^i : \underline{\underline{E}} + M^{ij} p^j \end{cases}$$

Where $\underline{\underline{\Sigma}}$ is the macroscopic stress, $\underline{\underline{E}}$ is the macroscopic strain, φ^i is the porosity of the family of aggregates i in deformed configuration, f^i is its porosity in undeformed configuration, $\mathbb{C}^{hom}$ is the homogenized stiffness tensor, $\underline{\underline{B}}^i$ is the Biot coefficient of family i, and M^{ij} is the crossed Biot compliance between families i and j.

To make this description fully operational, a few more elements are needed. First, the volume equilibrium of the gel in the porosity surrounding each aggregate family is written, giving the relation between the attack depth $\alpha^i(t)$ and the pressure as well as the external loads. As long as the porosity of the attacked zone of the aggregate and the ITZ are not filled with gel, the pressure remains zero.

Second, the matrix of Biot compliances is assumed to be diagonal. Physically, that means that the pressure build-up occurring in a given aggregate family has a negligible influence on the porosity volume of another family. Quantitative arguments have been given in [11] to back-up this assumption.

2.3 Micromechanical computation of the homogenized properties

The key point to take the cracking state into account is to be able to compute the macroscopic poromechanical coefficients of Equation (1) as functions of the cracking state. This requires studying all possible configurations and computing their homogenized properties: stiffness tensor, Biot coefficients, Biot compliances.

In our work, this was performed by using the micromechanics estimate proposed by Zheng and Du [12]. Two main morphologies have been examined. First, the case of the attacked aggregate without decohesion and without cracking. In this case, each pattern consists of concentric spheres, in which the constitutive behaviour is poroelastic, embedded in the cement paste matrix. To write the localization tensors of this pattern, a closed-form solution by Love solution was used [13]. Second, the case of the attacked aggregate which has undergone decohesion from the cement paste matrix, and possibly cracking in the cement paste. To write the localization tensors corresponding to this situation, an approximate combination of the localization tensors of a sphere and cracks was proposed, and validated through 2D finite element simulations, allowing to have a closed-form expression for the localization tensor of the cracked cavity.

2.4 Energy criterion

Once the morphology of the attacked medium has been described and the scenario of cracking has been assumed, a methodology was developed to initiate and propagate the cracks considered in the model. The choice that was made when building the model is that of using an energy criterion. According to this criterion, the creation of cracks dissipates energy, and this energy is provided either by the release of elastic energy, or by the boundary conditions (which means that the potential energy is used) [14].

Another assumption, in the spirit of Griffith's criterion, is that the creation of cracks provides energy proportionally to the crack surface. Since some materials or regions of concrete are less hard than others, this energy can be different depending on the location of the crack. In the current model, two regions are affected by cracking: the aggregate/cement paste interface (ITZ) and the cement paste itself. These crack surfaces have surface energies called G^{dec} and G^{fiss}. The dissipated energy during the evolution of the cracking state is simply, for a given aggregate family, proportional to its volume fraction in the concrete, and to the sum of the surface of the aggregate multiplied by G^{dec} and of the surface of the annular cracks multiplied by G^{fiss}.

Concerning the released energy, it has to be computed from the elastic energy and from the work of the boundary conditions. The elastic energy can be written easily thanks to the poromechanical description of the medium. The contribution of the solid skeleton of the porous medium, at a given macroscopic strain and given pressures in the aggregate families writes:

$$(2)\quad E_{el,ske}^{\underline{\underline{E}},p^i} = \frac{1}{2}\underline{\underline{E}} : \mathbb{C}^{hom} : \underline{\underline{E}} + \frac{1}{2}\sum_{i=1}^{N_f} (p^i)^2 \mathrm{M}^{ii}$$

While the contributions of the gel and of the remaining part of the aggregate after decohesion are not recalled but are straightforward to write.

Finally, the energy criterion is formulated as a problem of minimization of the total energy (sum of the potential and of the dissipated energy for a given set of loading parameters and a given set of crack sizes).

3 VALIDATION OF THE MODEL ON LABORATORY RESULTS

The model has been validated by reproducing Multon's experiments [8]. In this work, reactive and unreactive concrete cylinders were tested, and nine different boundary conditions were used. In the axial direction, the applied load was set equal to 0 MPa, 10 MPa, and 20 MPa and the strain was measured, using creep frames. In the radial direction, the sample was left free of stress, or restrained using 3 mm or 5 mm steel rings, which were equipped with wire strain gages in order to determine the radial strains and stresses.

The attack depth of all aggregates was assumed to be the same at a given time, and to evolve in time as its square root, to account for the fact that diffusion of alkali in the aggregates is assumed to be the phenomenon driving the kinetics of the attack.

The cracking energy in the cement paste was assumed to be twice than that in the ITZ, in order to reduce the number of parameters to identify. Finally, two experiments out of nine were used to identify the bulk modulus of the gel, its expansion factor, the width of the ITZ, the cracking energy, and the speed of the dissolution front into the aggregates.

The measurements and predictions for the strain in the nine experiments are shown on Figure 3. The agreement between the predictions of the model and the measurements is good up to 10 MPa. For the 20 MPa loading, the load is so important that decohesion could not occur without inducing the interpenetration of the aggregate and the cement paste matrix. No contact was implemented, allowing cracking without interpenetration, but interpenetration was forbidden. Therefore, the progress of damage is blocked under high compressive loads. One sees that the model in its current version should not be used for loads higher than 10 MPa.

Stresses have been reasonably well predicted as well, as illustrated in Figure 4. The same difficulties appear for loads higher than 10 MPa. One believes that these could only be solved by implementing a model of partial decohesion, or full decohesion with contact.

4 APPLICATION OF THE MODEL TO AFFECTED PILLARS

At the end of the PhD thesis of the author, the model (initially developed in Matlab), was translated into Python and implemented into the 'Materials Ageing Platform' which is a simulation platform (developed at EDF R&D MMC) with the help of Charles Toulemonde [15]. Hence, the model was available for the use on specific industrial cases at EDF. The model was applied to a specific case of swelling reaction of columns in a French nuclear plant. These structural members are part of a cooling tower with a very specific design, which was built in 1979. The dimensions of the columns are very impressive: a diameter of 70 cm, and a length of 18 m. Their number also is impressive, since a hundred of them bear the load of a large reinforced concrete slab with a diameter larger than 100 m and a number of very large fans (see Figure 5).

4.1 Signs of swelling reaction

The columns were built on site, with aggregates from the region on the nuclear plant. One of the two sands in the fraction 0 to 1.25 mm is considered potentially reactive. At the same time, to guarantee a fast setting of concrete in a single mould for all the columns, heating was applied (mostly during winter). The temperature reached 65°C during casting.

Since the role of the cooling towers is to optimize the heat exchange between air that is extracted and water that is spread at the periphery of the structure, there is a constantly warm and moist environment during operating of the plant: between 30°C and 35°C, and 100% RH.

This environment, as well as the presence of reactive aggregate and heating during setting, are very likely to threshold the occurring or ASR and DEF. In 2007, vertical cracks were seen on some of the columns. Some very rare traces of corrosion could also be seen. Afterwards, a swelling reaction was suspected, and studies were undergone to assess the remaining load bearing capacity of the members.

The loading of the pillars is quite well known. There are three main vertical loading magnitudes: 1.3 MPa, 2.3 MPa, and 2.8 MPa.

Cores were extracted from some of the cracked pillars, and their residual expansion was tested with procedures adapted to ASR and DEF. In both cases, the magnitude of the expansion was moderate to low. Microscopy analysis showed the presence of massive ettringite and also of alkali-silica gel. It was not possible to fully conclude which of these two reactions was the main responsible

of the degradations. Moreover, two main risks were identified concerning the structure: the buckling of the columns due to a decrease of the Young's modulus of the attacked concrete, or the yielding and rupture of stirrups which could trigger the buckling of the vertical rebars, and thus cause the failure of the column itself. Concerning the first risk, since the design of the columns is very conservative, it was not considered urgent to undertake actions. Concerning the second risk, it was decided to reinforce some of the columns with carbon FRC of thickness 0.55 mm and Young's modulus 76.8 GPa.

4.2 Calibration of the model parameters

Unfortunately, no strain measurement mechanism was used since the beginning of the service life of the pillars. Therefore, it is very difficult to know the kinetics and the amount of swelling reached today. Only very few information can be used for the calibration of the model:

- The evolution of the crack opening was measured on about 20 vertical cracks on the columns, for a period of five years. Since these vertical cracks align with the vertical rebars, and since there are 6 of these vertical rebars for all members, it is possible to determine very approximately the speed of swelling of the column in the radial direction. The idea is to assume that the 6 cracks open at the same pace as the one that is measured, and that the skin of the concrete does not expand at all. Since most columns only have 2 or 3 vertical cracks, this gives us an upper bound for the radial speed of the swelling.
- Another information of importance is that of the longitudinal strain. No measurement was made, but we know that some horizontal cracks have been detected on some of the columns in 2013 or 2014. This information was used, along with an estimation of the magnitude of basic creep from tests by Kommendant [16] on a similar concrete at various temperatures and loaded at 28 days, and the assumption that the skin of concrete is not submitted to the swelling reaction, nor creep. Since the loading time is much earlier, one thinks that this gives an upper bound for the vertical creep and hence, swelling reaction strain.
- Another information that was available but could not be used was the results from residual expansion tests on cores from the affected columns. The environment is so different that it is hard to use these as an indication for kinetics, and the result of total residual expansion was not available at the time of completion of this work.

Few additional information was available about the concrete of these pillars. The aggregate size distribution was taken from [17], and aggregate sizes from 0 mm to 1.25 mm were considered as reactive. The total volume fraction of aggregate was taken equal to 75%, including 10% of reactive aggregates. The fraction of reactive silica in the aggregates was set to 0.1. The Young's modulus of sound concrete is known to be around 33 GPa.

The model parameters were calibrated so as to find the correct Young's modulus for the sound concrete, and to respect the speed of radial expansion and the estimated current value of vertical expansion. The pillars loaded at 2.3 MPa without FRC reinforcement are used for the calibration. The strains are shown on Figure 6, while the strain rates are shown on Figure 7. Since there is no other measurements available, no further validation of the model can be made for this specific case.

4.3 Results

The model has been used with the parameters identified previously. A first question that required investigation and thus motivated part of the study is the difference of vertical expansion among columns with different loadings. The large slab which is carried by the columns, when appraised from above, shows cracking right above the point where it rests on the least loaded column. Hence, there was a suspicion that the expansion of these members was more important, and thus it induced flexion and cracking in the slab.

According to the present model, the displacements of the head of the columns lies between 0 cm for the most loaded members, and 2.4 cm for the least loaded members (see Table 1). This difference seems large enough to explain the appearance of cracks in the slab. The quantification of these displacements helped understanding the overall behaviour of the structure and gave consistency to many observations in the field: vertical and horizontal cracks on the columns, as well as cracks on the upper face of the slab above the columns bearing the lightest loads.

The model also yields predictions on the loss of Young modulus. The Young moduli predicted by the model are the lower bound for the true moduli, due to the simplicity of the model on at least two points. First, the gel is assumed liquid, whereas due to incorporation of calcium, it is likely to get closer to a solid while ageing. Second, creep it not accounted for at the microscopic scale, which induces an overestimation of the microscopic damage for a given expansion [6]. The decrease of the

Young modulus in the vertical direction, which is of interest in the purpose of verifying that the columns are still stiff enough to avoid buckling, is maximum for the least loaded pillars, and of 39 %.

Finally, the last objective of this study was to verify if the FRC composite that had been installed on the columns could impose a significant radial confinement to the concrete, and also if this potential confinement could have detrimental effects by redirecting expansions to the vertical direction, and perhaps increase the phenomenon of cracking of the slap supports by the pillars. Even without taking into account the creep of the FRC (which is enhanced by heat and humidity in the cooling tower), it was found that the confinement provided by the FRC is negligible. This information helped changing the maintenance program for the columns, by focusing on preventing the ingress of water in concrete instead of providing mechanical restraint.

4.4 Discussion

The main difficulties with this application of the model to a real case were the fact that the swelling reaction was not clearly identified (indications that there might be both ASR and DEF), and that there was very little strain measurements performed on the structure. These two difficulties are probably faced very frequently when modelling ongoing ASR or DEF in a real structure is attempted.

The question which must then be asked is: can we trust the results given by the model, since the mechanism involved in the real structure might be quite different from the mechanisms described in the model, and that the calibration of the parameters is performed on very little data, while no true validation on other data could be attempted. The approach used in this paper to answer these doubts was to use upper bound values for the strains and strain rates that were used to identify the parameters of the model.

Since one must very cautiously use predictions of such a model, the results presented here were mostly used to justify that there is no advantage of reinforcing the pillars mechanically (at least at this level of stiffness of the reinforcements). Concerning the future monitoring of the structure, an ambitious program of measurements of the first eigen-frequency of the columns has been proposed and is now being implemented. The goal will be to enable the detection of buckling risks by the reduction of the first eigen-frequency of the pillars.

5 CONCLUSIONS

In this article, we present a model aiming at predicting the evolution of the homogenized properties of concrete undergoing ASR, from a microscopic description of the cracking of the ITZ and the cement paste. A specific focus was placed on the anisotropy of swelling and damage due to the load applied on the affected concrete. This model is based on micromechanics, poromechanics, and on an energy criterion.

A validation of the model on laboratory experiments is then presented. It shows the model is able to predict the orientation of cracking and its consequences in terms of anisotropic expansions.

Finally, the model is used for an industrial application at EDF. Columns which are affected by a swelling reaction are modelled. The results obtained show that columns with different loads can elongate quite differently, with an estimation of the elongation difference of about 2 cm, which explains cracking observed in the slab which is supported by the columns. Another important conclusion is the very small confinement that is brought by the FRP that was installed to prevent water ingress and for safety in the very unlikely case of yielding and rupture of a stirrups.

ACKNOWLEDGEMENTS

The development of the model was funded by the 'Chaire durabilité des matériaux et des structures pour l'énergie' at ENPC, France. The work was supervised by Prof. Alain Ehrlacher.

6 REFERENCES

[1] J. Ponce (2006): Different manifestations of the alkali-silica reaction in concrete according to the reaction kinetics of the reactive aggregates, Cement and Concrete Research, vol. 36, pp. 1148-1156.

[2] S. Poyet, A. Sellier, B. Capra, G. Foray, J.-M. Torrenti and H. E. Cognon (2007): Chemical modelling of alkali-silica reaction: influence og the aggregate size distribution, Materials and Structures, vol. 40, pp. 229-239.

[3] E. Grimal, A. Sellier, Y. Le Pape and E. Bourdarot (2008): Creep, shrinkage, and anisotropic damage in alkali-aggregate reaction swelling mechanism - Part I: Constitutive model, ACI Materials Journal, vol. 105, no. 3, pp. 227-231.

[4] V. Saouma (2013): Numerical Modeling of Alkali Aggregate Reaction, CRC Press.

[5] Z. Bazant, G. Zi and C. Meyer (2000): Fracture mechanics of ASR in concretes with waste glass particles of different sizes, Journal of Engineering Mechanics, vol. 126, no. 3, pp. 226-232.

[6] A. Giorla and K. Scrivener (2015): Influence of visco-elasticity on the stress development induced by alkali-silica reaction reaction, Cement and Concrete Research, vol. 70, pp. 1-8.

[7] L. Sanchez, B. Fournier, M. Jolin and J. Duchesnes (2016): Reliable quantification of AAR damage through assessment of damage rating index (DRI), Cement and Concrete Research, vol. 67, pp. 74-92.

[8] S. Multon and F. Toutlemonde (2006): Effect of applied stresses on alkali-silica reaction-induced expansions, Cement and Concrete Research, vol. 36, no. 5, pp. 912-920.

[9] D. Hobbs (1988): Alkali-silica reaction in concrete, London: Thomas Telford.

[10] L. Charpin (2013): Modèle micromécanique pour l'étude de la réaction alcali-silice, Université Paris Est, France.

[11] L. Charpin and A. Ehrlacher (2014): Microporomechanics study of anisotropy of ASR under loading, Cement and Concrete Research, vol. 63, pp. 143-157.

[12] Q.-S. Zheng and D. D.-X. (2001), An explicit and universally applicable estimate for the effective properties of multiphase composites which accounts for inclusions distribution, Journal of the Mechanics and Physics of Solids, vol. 49, pp. 1781-1811.

[13] A. Love (1927): A treatise on the mathematical theory of elasticity, Fourth Edition, Cambridge University Press Warehouse.

[14] G. Francfort and J.-J. Marigo (1998): Revisiting brittle fracture as an energy minimization problem, Journal of the Mechanics and Physics of Solids, vol. 46, no. 8, pp. 1319-1342.

[15] F. Latourte, C. Toulemonde, J.-F. Rit, J. Sanahuja, N. Rupin, J. Ferrari, H. Perron, E. Bosso, A. Guery, J.-M. Proix and B. Watrisse (2013): The materials ageing platform: towards a toolbox to perform a wide range of research studies on the behavior of industrial materials, Montpellier, France.

[16] G. Kommendant, M. Polivka et D. Pirtz (1976): Study of concrete properties for prestressed concrete reactor vessels, Final Report No. UCSESM 76-3 (to General Atomic Company), Berkeley: Department of Civil Engineering, University of California.

[17] A. Neville (2000), Propriétés des bétons, Eyrolles.

TABLE 1: Vertical strains, length change and radial strain predicted by the model at an age of 30 years.

Load	**1.3 MPa**	**2.3 MPa**	**2.8 MPa**
Vertical strains	0.12%	0.02%	0%
Length change (on 20 m)	2.4 cm	0.4 cm	0 cm
Radial strains	0.01%	0.05%	0.07%

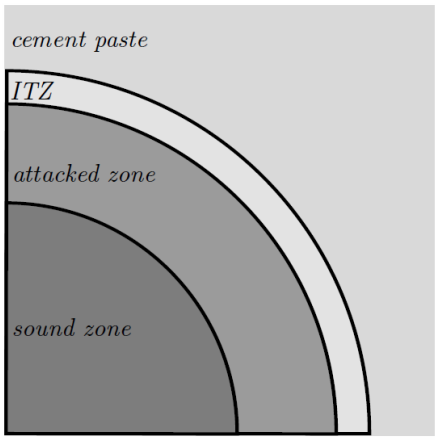

FIGURE 1: Schematic attack of an aggregate.

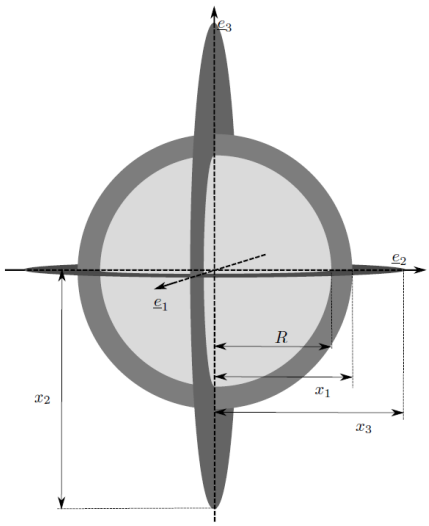

FIGURE 2: Spherical cavity surrounded by three orthogonal cracks.

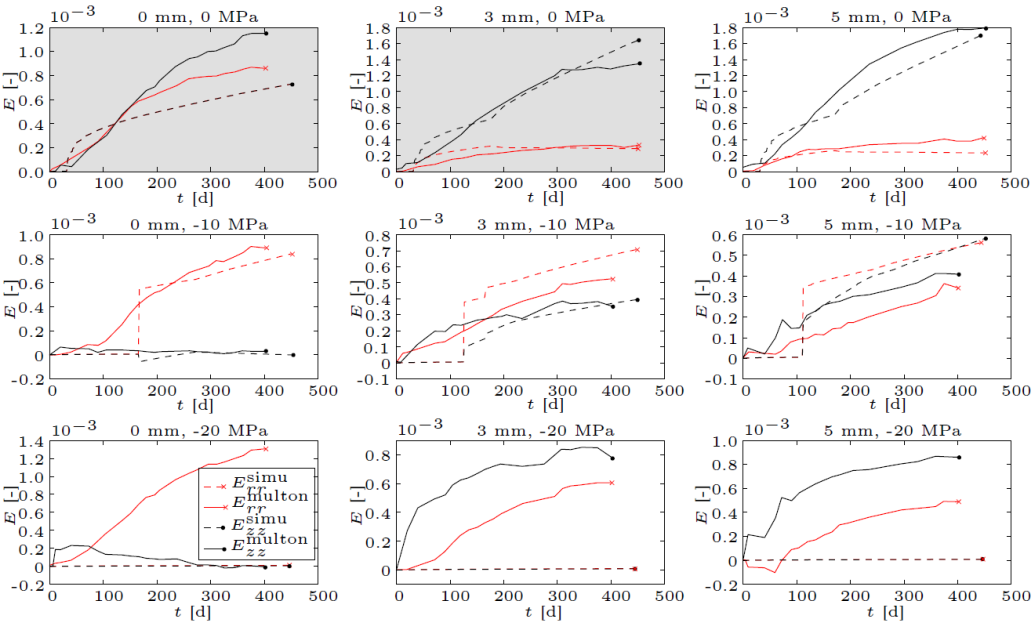

FIGURE 3: Identification of parameters on Multon's experiments. Strain. Grey plots: experiments used for the identification.

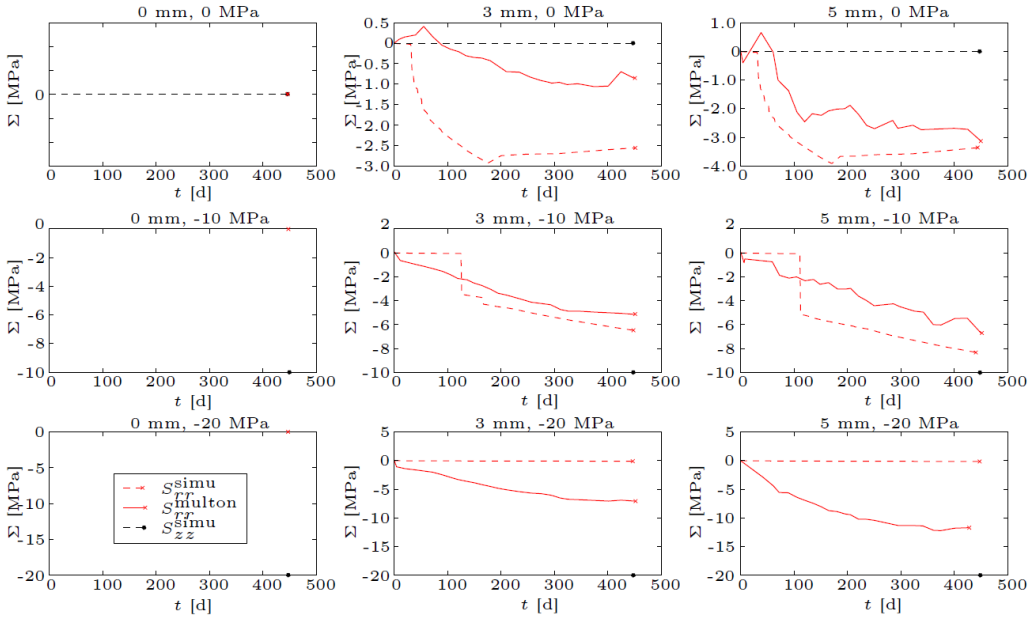

FIGURE 4: Predicted stresses compared to Multon's measurements.

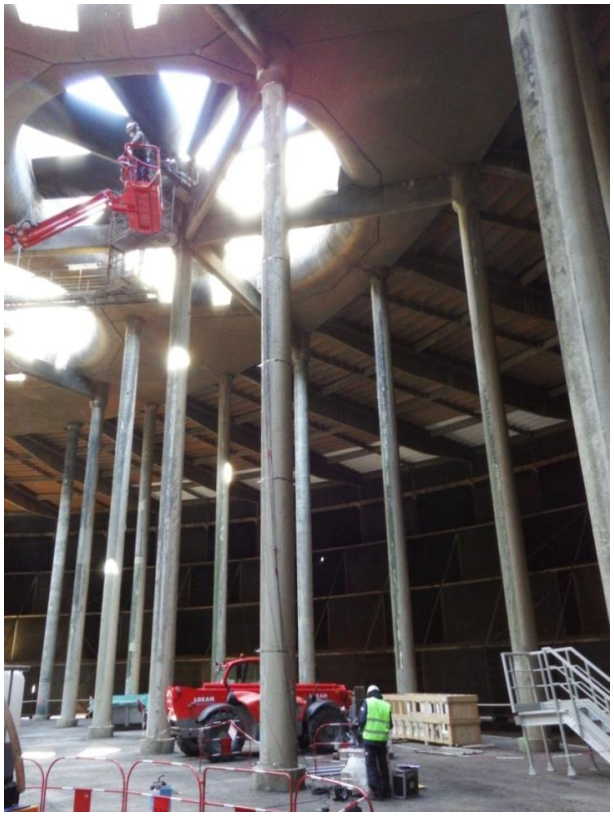

FIGURE 5: A view of some of the pillars and the concrete slab with one of the fans.

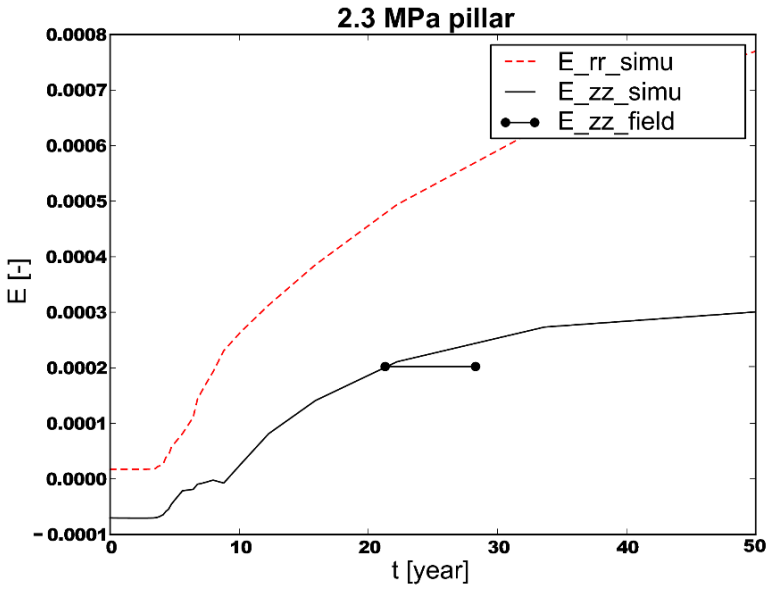

FIGURE 6: Predicted radial and longitudinal strains compared to the estimated field longitudinal strain.

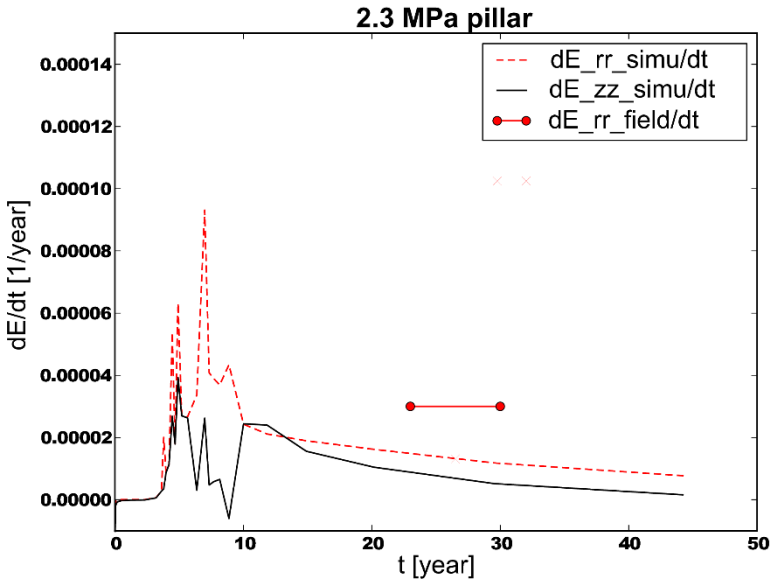

FIGURE 7: Simulated strain rates compared to the speed of deformation determined from field crack opening measurements.